Planar Metamaterial Transverse Equivalent Network and Its Application to Low-Profile Antenna Designs

A. Vallecchi[§1], M. Albani[#2], F. Capolino[*3]

[§]*Department of Electronics and Telecommunications, University of Florence, 50100 Florence, Italy*
[1]andrea@lam.det.unifi.it

[#]*Department of Information Engineering, University of Siena, 53100 Siena, Italy*
[2]matteo.albani@ing.unisi.it

[*]*Department of Electrical Engineering and Computer Science, University of California, Irvine, CA 92697-2625, USA*
[3]f.capolino@uci.edu

***Abstract*— We present a lumped circuit description of a novel metamaterial layer made of arrayed pairs of tightly coupled conductors (dogbones or Jerusalem crosses). This lumped element network is synthesized to exhibit the same frequency response of the metamaterial layer when inserted in the plane-wave equivalent transmission line. The metamaterial and its transverse equivalent network (TEN) model is then applied to the design of a high impedance surface for low profile dipoles and a partially reflective superstrate for highly directive Fabry-Perot cavity antennas. Numerical results illustrating the radiation properties of such antennas are provided.**

I. INTRODUCTION

As an alternative to conventional split-ring resonator based negative index materials [1], [2], pairs of finite-length wires have been recently suggested as constitutive particles for creating a medium with an effective negative refractive index [3], [4]. The pairs of coupled conducting wires exhibit both a magnetic resonance (antisymmetric mode) and an electric resonance (symmetric mode) that can be properly tuned to the desired frequency by adjusting the length of the pair. Later on, the cut-wire pair arrangement has been further elaborated and the adoption of dogbone-shaped conductors in place of simple cut-wires has been proposed to achieve enhanced control on the particle resonances [5], [6] and reduce the size of the metamaterial unit cell.

An approximate method to predict the magnetic resonances f_m of metamaterials composed of pairs of dogbone conductors has been proposed in [6]. However, such formulas, based on a transmission line (TL) model of the antisymmetric mode in the pair of central stripes of each dogbone, completely neglect the fringe capacitances at the TL ends and bends, and the capacitance between contiguous particles. Yet, for larger thickness of the dielectric substrate supporting the dogbone conductors (H), the fringing effects and coupling between adjacent cells become pronounced. The latter interaction affects not only the electric but also the magnetic resonance, especially in the case of large separation H between the top and bottom conductors compared to the distance between contiguous conductors. As a result, at small values of H, the f_m approximations developed in [6] are in good agreement with results of numerical simulations. On the contrary, at large values of H, the rapid variation of f_m cannot be explained in terms of this simple TL model for a *single isolated* particle because the fringing effects and coupling between particles strongly influence the collective response of the whole array.

In this work we present a lumped element description of a metamaterial layer made of pairs of conductors. By postprocessing the reflection and transmission coefficients calculated by using a full-wave code, a lumped element network is synthesized that exhibits the same frequency response when inserted in the plane-wave equivalent TL. The presence in the metamaterial response of both an electric (symmetric) and a magnetic (antisymmetric) resonance finds its correspondence in two respective resonant LC groups arranged in an equivalent balanced X-network. The equivalent network is useful for a quick numerical description of the layer but also reveals the physical operating mechanism of the metamaterial dictated by particle interactions.

First, we analyse propagation through the new metamaterial in planar technology. We show that the reflection and transmission features of a periodic array of dogbone pairs as well as the dispersion diagram are accurately predicted by this simplified model. The equivalent circuit is used in a transverse equivalent network (TEN) model of low-profile antennas. In particular we will use the metamaterial (a) to design a high impedance substrate for locating dipole antennas, and (b) also to design a superstrate for high gain Fabry-Perot cavity (FPC) antennas. By using the TEN model, the radiation properties of such antennas are analysed. Numerical simulations will also support the theory.

II. METAMATERIAL IN PLANAR TECHNOLOGY

The planar metamaterial is made of arrayed pairs of metallic conductors with a dogbone shape (Fig. 1). Because of the tight coupling of the two conductors, two working regimes can be excited: the symmetric and the antisymmetric current mode distributions. The antisymmetric mode, also called TL mode, has been associated to artificial magnetism, since each antisymmetric current forms a loop that can be associated to an equivalent magnetic dipole oriented along the y-direction.

A layer of arrayed pairs exhibits complex transmission and reflection spectra because of the interplay of the two kinds of resonant modes that can be excited. It has been shown that a

stack of layers may exhibit a negative index of refraction and thus it supports a backward-wave travelling across them. Furthermore, we show here that the characteristic impedance of each layer can be engineered to provide a high impedance material.

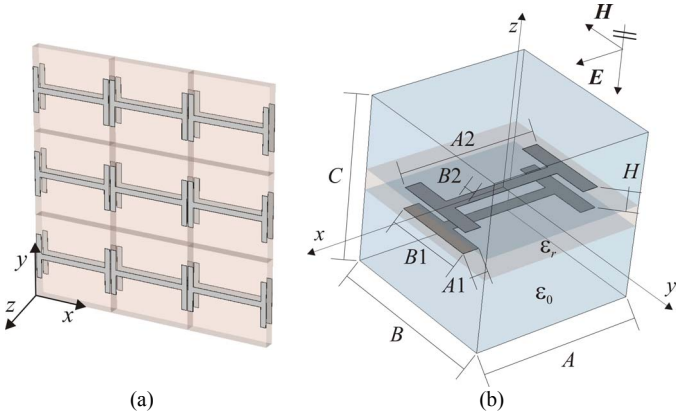

Fig. 1 (a) Perspective view of a layer of the metamaterial formed by a periodic arrangement of tightly coupled pairs of dogbone-shaped conductors printed on a dielectric substrate. (b) Metamaterial elemental particle (unit cell) with geometrical parameters quoted. The polarization of the incident electric field is along the *x*-direction.

The TL model consists in replacing the layer of arrayed conductor pairs by the equivalent 2-ports network shown in Fig. 2, made by lumped physically realizable circuital elements. Neglecting losses both in the conductors and the dielectric substrate, the impedances of the equivalent X-network are only made by *L*-*C* elements that take into account both the electric and magnetic resonances characterizing the metamaterial response. As shown in Fig. 2, the magnetic resonance is described by a parallel *LC* resonator [6], whereas the electric resonance, as the usual stop band of capacitive FSSs, is described by a series *LC* resonator.

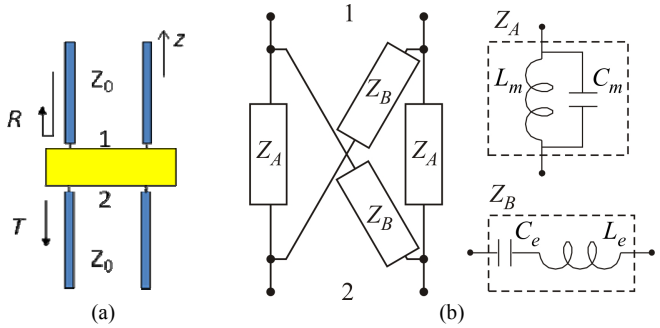

Fig. 2 Equivalent network for the metamaterial layer made of arrayed pairs of dogbone-shaped conductors and its inclusion in a TL model.

As an example, we consider the response of a layer of dogbones pairs printed on a dielectric substrate with $\varepsilon_r = 2.2$ (e.g., RT Duroid 5880). The various geometrical parameters characterizing the unit cell of the considered metamaterial (cf. Fig. 1 (b)) are as follows (in mm): $A = 7.5$, $B = 7.5$, $A1 = 0.5$, $B1 = 4$, $A2 = 7.4$, $B2 = 0.5$, $H = 1.0$. The dimension of the unit cell along the *z*-direction is $C = 8.0$ mm, and therefore ports are defined at $z = \pm 4$mm. The magnitude and phase of the reflection coefficient R in Fig. 3 predicted by the synthesized TL and X-network are in good agreement with those obtained numerically. The electric and magnetic frequencies are $f_m = 6.89$ GHz, and $f_e = 7.30$ GHz, respectively.

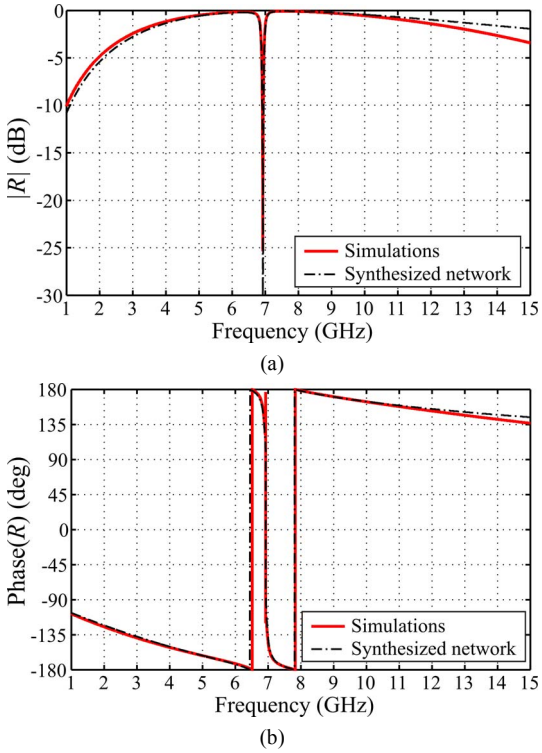

Fig. 3 Reflection coefficient vs. frequency for a layer of dogbones pairs: (a) magnitude; (b) phase. The *magnetic* resonance is at $f_m \approx 6.9$ GHz, whereas the *electric* resonance is at $f_e \approx 7.3$ GHz. Data from a numerical analysis are compared with those from our proposed equivalent network model.

III. Low Profile Dipole on a Reactive Impedance Surface

The objective here is to demonstrate that the developed equivalent circuit can be applied to the design of a low profile antenna consisting of a dipole located on top of a reactive impedance surface (RIS) [8]. The high impedance exhibited by the RIS permits to locate the metallic dipole very close to the surface itself without inhibition of the dipole radiation. Furthermore, the substrate prevents radiation from travelling across, resulting in a low profile antenna with high efficiency, even though the antenna system (comprising the dipole and thin metamaterial substrate) is integrated on top of a lossy structure. Indeed, this low profile antenna design is suitable for integration in supporting platforms like metallic structures or chips, where also active components could be assembled, and can be realized in CMOS technology. It is also suitable for wearable antennas that have the constraints of being flat and on thin flexible substrates that need to be simple to realize. Properly scaled, it can be designed for a large variety of frequency bands from microwaves to millimiter waves.

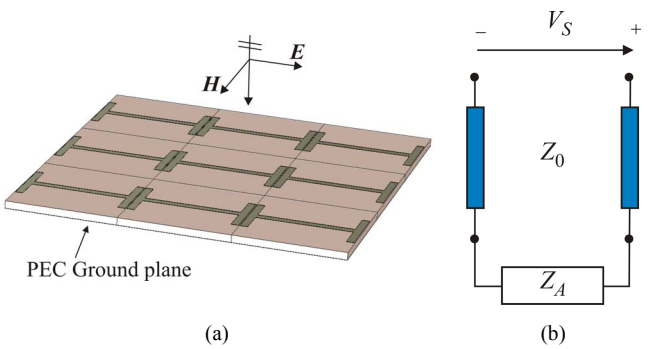

Fig. 4 (a) RIS substrate composed of a periodic array of dogbone-shaped conductors printed on a PEC-backed dielectric material and illuminated by a plane wave. (b) Circuit approach representation of the RIS.

An RIS structure composed of a periodic array of dogbones printed on a PEC-backed dielectric substrate with thickness H = 0.5 mm and permittivity $\varepsilon_r = 2.2$ is introduced (Fig. 4(a)). The geometrical parameters characterizing the unit cell of the considered periodic material are the same as in Fig. 2.

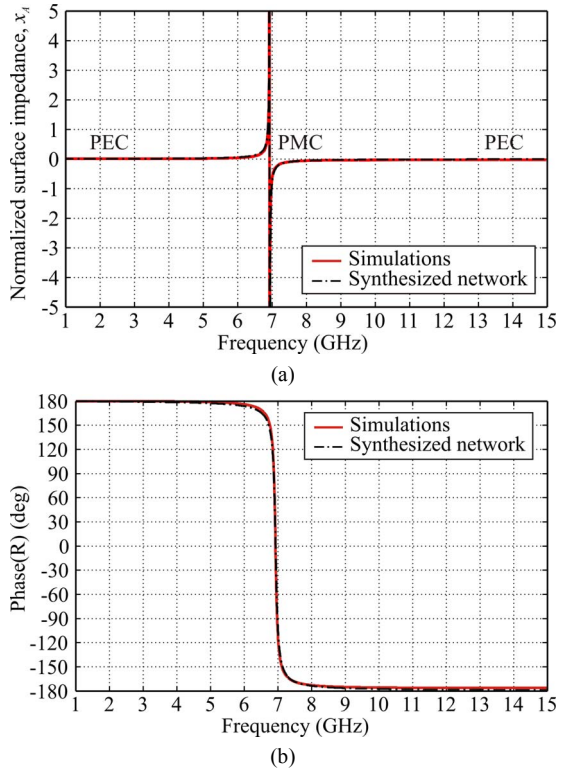

Fig. 5 Characteristics of the RIS substrate at normal incident determined utilizing the circuit approach and full-wave simulations. (a) Normalized surface impedance, and (b) reflection coefficient phase.

To facilitate the design procedure, a simple and yet very accurate circuit model for this structure is derived starting from the equivalent network developed for a metamaterial layer of dogbone pairs with dielectric substrate thickness twice that of the RIS ($2H$). In fact, in the hypothesis of illumination by two normally incident plane waves with antisymmetric polarization of the electric field, the original metamaterial layer can be split in two identical parts backed by a PEC plane, each of which corresponds to the considered RIS. Accordingly, the structure can be modelled using a TL approach as shown in Fig. 4(b).

The normalized surface reactance x_A ($jx_A = Z_A / Z_0$) of the RIS as a function of frequency is plotted in Fig. 5(a). Both data obtained from full-wave simulations (CST Microwave Studio) and the equivalent circuit are displayed, and the two set of results are in very good agreement. Moreover, the phase of the reflection coefficient R of the RIS at normal incidence as deduced from the circuit representation ($R = (Z_A - Z_0)/(Z_A + Z_0)$) and calculated by CST are shown in Fig. 5(b), and again an excellent agreement is observed. As apparent, this structure, depending upon the operating frequency, can behave as a capacitive or inductive RIS. The reactance is inductive at frequencies below resonance, open circuit at the resonance (behaving as an artificial magnetic conductor (AMC) surface) and capacitive above the resonant frequency. At frequencies much lower than the resonant frequency the RIS shows low impedance and acts as a PEC surface and at the resonance the reactance goes to infinity and the RIS behaves as a AMC.

We now examine the performance of a dipole over the RIS considered above; the geometry of the dipole over the finite-size RIS is shown in Fig. 6. The finite-size RIS is composed of a 8×8 array of dogbone-shaped conductors. The dipole antenna has length 20.6 mm and diameter-to-length ratio of about 0.01. The dipole is excited using a delta-gap source at the centre. The height of the dipole above the RIS is 1 mm and thus the total thickness of the antenna (including the dipole and the substrate) is 1.5 mm. The operating frequency of the dipole in free space is 6.75 GHz at which frequency its length is 0.46 λ.

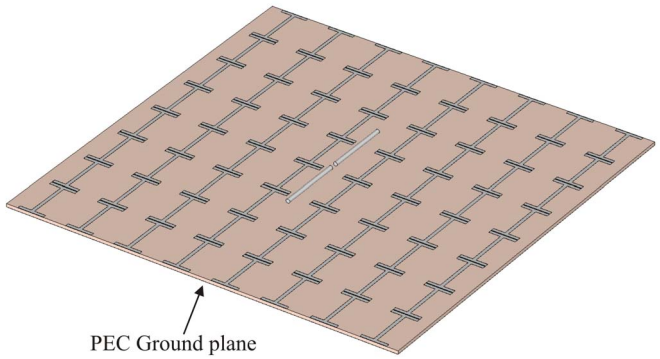

Fig. 6 Dipole antenna over the RIS substrate. RIS is a 8x8 finite array of dogbone-shaped conductors printed on a dielectric.

The input impedance and the radiation patterns of the antenna are obtained using CST MS and are shown in Fig. 7 Fig. 8, respectively. As demonstrated in Fig. 5(a), the RIS has a resonant frequency of about 6.9 GHz at which it acts like an AMC. Below this resonance the RIS is inductive. Because the dipole resonates at 6.75 GHz, below this frequency the dipole is capacitive. As a result the operating frequency of the dipole

over the RIS is at f = 6.3 GHz, rather below the free-space operating frequency 6.75 GHz. At this frequency the dipole length is 0.43 λ. Fig. 7 (b) shows the return loss of the dipole over the RIS, the operating bandwidth is small but it could be improved by increasing the thickness of the RIS. Referring to Fig. 8, the radiation pattern of the dipole over the RIS shows a remarkable front-to-back ratio of about 22 dB. Simulation results also show a gain of 7.7 dBi and a high radiation efficiency of 78 % (taking into account both ohmic and dielectric losses).

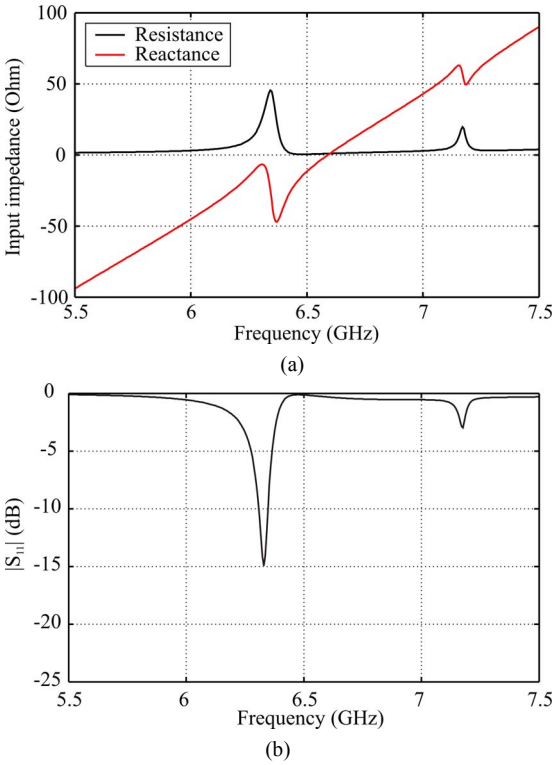

Fig. 7 Input impedance of dipole antenna over the RIS substrate: (a) input resistance and reactance and (b) return loss.

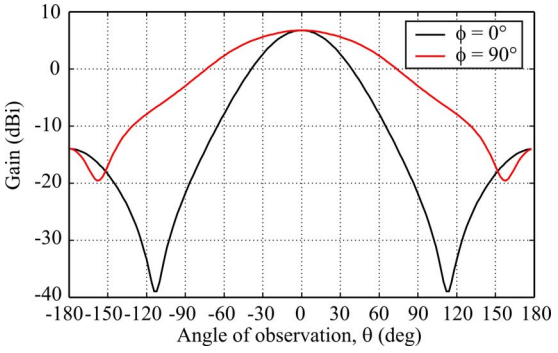

Fig. 8 Radiation patterns of dipole antenna over the RIS substrate.

IV. Low Profile Fabry-Perot Cavity Antenna

Highly directive antennas can be realized by using FPCs made of a ground plane covered by a partially reflective surface (PRS) [9]-[14]. FPC are often excited by a single feed but they are also useful in connection with array of feeds [15]. Here we show that when the novel kind of metamaterial layer is used as a PRS interesting properties arise.

A FPC is usually made by suspending a low impedance PRS about half-a-wavelength above a ground plane so as to form a resonant cavity whose field leaks from the top surface. The high directivity is achieved because the feed at the center of the antenna launches one or two radial leaky modes with low propagation and attenuation constants. These leaky wave antennas are also denoted as electromagnetic band gap (EBG) antennas. In recent years researchers have tried to make FPC antennas with two simultaneous frequencies of operation, i.e., the cavity has to resonate at different frequencies. Some of the past solutions are based on having two distinct PRS in the cavity, or one PRS over an engineered frequency selective "ground" plane. Here we present the design of a dual frequency FPC antenna based on using the same the layer of coupled dogbone metamaterial shown in Fig. 1. The antisymmetric mode supported by the structure introduces a novel behaviour for the PRS covering the FPC.

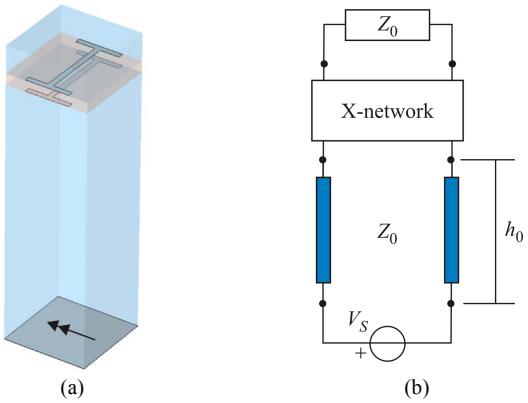

Fig. 9 (a) Geometry of the FPC antenna (only one cell of the periodic superstrate is shown) made by a layer of arrayed dogbone pairs, excited by a magnetic current over the ground plane. (b) Equivalent TL model.

Indeed, the dogbone pair layer presents a low impedance over a wide frequency band around its "electric resonance" and is suitable for realizing the PRS at the top of the FPC. In addition it exhibits a "magnetic resonance", associated to the antisymmetric mode supported by each pair, at which it becomes "transparent" and a sharp null in its reflection coefficient occurs (cf. Fig. 3). Such a feature creates an anomalous behaviour of the PRS reflection coefficient phase rapidly ranging a full 360° round in a narrow band around the magnetic resonance. As a consequence, the FPC resonance condition is met twice at two frequencies slightly below and above the magnetic resonance. This results in a dual-frequency behaviour for the FPC which exhibits its extraordinary gain at two close by frequencies. As an example we show the performances of a FPC for varying cavity height h_0. The gain for a magnetic dipole excitation of an infinite FPC whose unit cell is shown in Fig. 9(a) is determined by resorting to the TL model shown in Fig. 9(b) and a spectral

plane wave representation of the associated Green's function, which is calculated by a numerical integration as in [15]. The cavity height h_0 dictates the two FPC resonance frequencies around the magnetic resonance at f_m = 6.89 GHz, where the PRS is transparent and the gain is that of a grounded magnetic dipole independently of h_0. A tuning on h_0 set the two FPC resonance frequency with the same amplitude of the PRS reflection (and transmission) coefficient, and in turn the same FPC gain of about 23 dB; namely, h_0 = 22 mm corresponds to f_1 = 6.732GHz and f_2 = 7.062GHz for which $|T(f_1)| \approx |T(f_2)| \approx -10\text{dB}$. The radiation patterns in the two principal planes are also reported in Fig. 11. A narrow broadside beam is achieved at both the frequencies.

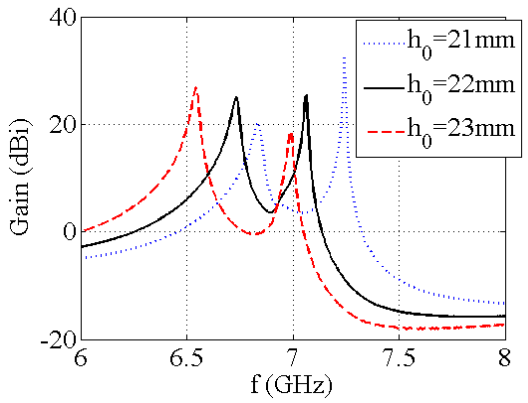

Fig. 10 Broadside gain vs. frequency for the FPC in Fig. 9(a), for different values of the cavity height h_0.

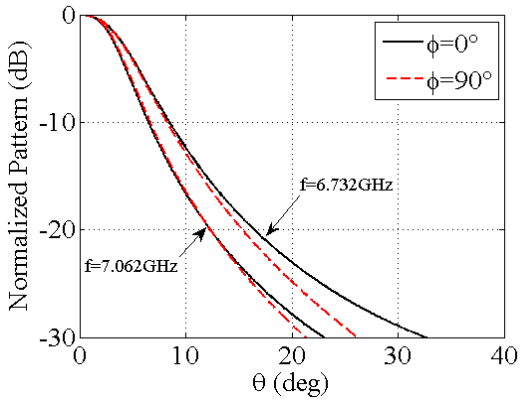

Fig. 11 FPC radiation patterns in the principal planes, at the two resonance frequencies f_1 = 6.732GHz and f_2 = 7.062GHz, for h_0=22mm.

CONCLUSIONS

In this paper we have shown how a metamaterial that can be easily arranged as planar substrates or superstrates is used to design low profile antennas. In particular, two examples have been shown.

First the metamaterial has been engineered to exhibit a high impedance and a low profile antenna consisting of a dipole in close proximity of the high impedance ground plane is designed, with a total thickness of 1.5 mm.

Also, a highly directive FPC antenna has been designed by using a metamaterial layer as the cavity superstrate. In this case, we have shown that a dual frequency behaviour is achieved at two near frequencies where the FPC enhances a magnetic dipole gain up to 23 dB with a narrow pencil beam in the broadside direction.

REFERENCES

[1] J. B. Pendry, A. J. Holden, D. J. Robbins, and W. J. Stewart, "Magnetism from conductors and enhanced nonlinear phenomena," *IEEE Trans. Microw. Theory Tech.*, vol. 47, no. 11, pp. 2075–2084, Nov. 1999.

[2] D. R. Smith, W. J. Padilla, D. C. Vier, S. C. Nemat-Nasser, and S. Schultz, "Composite medium with simultaneously negative permeability and permittivity," *Phys. Rev. Lett.*, vol. 84, pp. 4184–4187, 2000.

[3] V. M. Shalaev, W. Cai, U. K. Chettiar, H. Yuan, A. K. Sarychev, V. P. Drachev, and A. V. Kildishev, "Negative index of refraction in optical metamaterials," *Optics Lett.*, vol. 30, no. 24, pp. 3356–3358, Dec. 2005.

[4] J. Zhou, E. N. Economou, T. Koschny C. M. Soukoulis, "Unifying approach to left-handed material design," *Optics Lett.*, vol. 31, no. 24, pp. 3620–3622, Dec. 2006.

[5] J. Zhou, T. Koschny, L. Zhang, G. Tuttle, and C. M. Soukoulis, "Experimental demonstration of negative index of refraction," *Appl. Phys. Lett.*, vol. 88, p. 221103, 2006.

[6] G. Donzelli, A. Vallecchi, F. Capolino, and A. Schuchinsky, "Anisotropic metamaterial made of paired planar conductors: particle resonances, phenomena and properties," *Metamaterials.* (*Elsevier*), vol. 3, no. 1, 2009.

[7] A. Vallecchi, F. Capolino and A. Schuchinsky, "2-D Isotropic Effective Negative Refractive Index Metamaterial in Planar Technology," *IEEE Microwave and Wireless Components Letters*, vol. 19, 2009.

[8] H. Mosallaei, K. Sarabandi, "Antenna miniaturization and bandwidth enhancement using a reactive impedance substrate," *IEEE Trans. Antennas Propagat.*, vol.52, no.9, pp. 2403-2414, Sept. 2004.

[9] G. Von Trentini, "Partially reflecting sheet arrays," *IEEE Trans. Antennas Propagat.* Vol. 4, pp. 666-671, 1956.

[10] D. R. Jackson and N. G. Alexópoulos, "Gain enhancement methods for printed circuit antennas" *IEEE Trans. Antennas Propagat.*, Vol. 33, N.9, Sept. 1985.

[11] M. Thévenot, C. Cheype, A. Reineix, and B. Jecko, "Directive photonic bandgap antennas," *IEEE Trans. Microwave Theory Tech.*, 47, pp. 2115–2122, Nov. 1999.

[12] A. P. Feresidis and J. C. Vardaxoglou, "High gain planar antenna using optimised partially reflective surfaces," *IEE Proc. Microw. Antennas Propag.*, Vol. 148, pp. 345-350, 2001.

[13] T. Zhao, D. R. Jackson, J. T. Williams, H. Y. Yang, and A. A. Oliner, "General Formulas for 2-D Leaky-Wave-Antennas" *IEEE Trans. Antennas Propag.*, vol. 53, no. 11, pp. 3505–3514, Nov. 2005

[14] G. Lovat, P. Burghignoli, and D. R. Jackson, "Fundamental properties and optimization of broadside radiation from uniform leaky-wave antennas," *IEEE Trans. Antennas Propagat.,* Volume 54, Issue 5, pp. 1442-1452, May 2006.

[15] R. Gardelli, M. Albani, and F. Capolino, "Array thinning by using antennas in a Fabry-Perot cavity for gain enhancement," *IEEE Trans. Antennas Propagat.,* V. 54, N. 7, pp. 1979-1990, July 2006.